Determination of the Electron Transfer Mechanism through Decomposition of the Density Matrix

ARTICLE *in* THE JOURNAL OF PHYSICAL CHEMISTRY B · NOVEMBER 2004

Impact Factor: 3.3 · DOI: 10.1021/jp045641l

1 AUTHOR:

Eunji Sim
Yonsei University
60 PUBLICATIONS **828** CITATIONS

SEE PROFILE

Determination of the Electron Transfer Mechanism through Decomposition of the Density Matrix

Eunji Sim*

Department of Chemistry, Yonsei University, 134 Sinchondong Seodaemungu, Seoul 120-749, Korea

Received: September 25, 2004; In Final Form: October 23, 2004

We present a modified Feynman and Vernon's path integral formalism which allows independent consideration of coherent superexchange and incoherent hopping pathways of charge transfer processes in order to determine the type of transport mechanism. By classifying the pathways between donor and acceptor into different mechanisms and by decomposing the density matrix of donor−bridge−acceptor triads into corresponding partial matrices, the contribution of each mechanism is obtained separately. Numerical tests confirm that the scheme is valid and efficient in exploring the transport mechanism and that the incoherent hopping mechanism tends to govern charge transfer processes even in systems with high-energy bridge states.

1. Introduction

One of the long-standing issues in electron transfer (ET) is to figure out the transport mechanism of charge traveling between redox states.[1,2] Electrons may transfer from donor to acceptor through a direct route, which is called the superexchange pathway. On the other hand, the charge transport may be mediated by bridge states that are located between donor and acceptor, that is, through incoherent hopping pathways. In the superexchange mechanism, bridges solely serve to mediate donor and acceptor wave functions as a virtual bridge, while in the incoherent hopping mechanism, an electron is located on the bridge for a short time during its journey. Elucidation of the transport mechanism would have tremendous impact on various electronic devices and systems such as molecular wires[2,3] and biological,[4,5] organic, and inorganic[1,6] ET systems, in which an ET process characterizes chemical, biological, and electrical properties and functions. To understand the ET processes in the aforementioned systems, it is necessary to investigate the roles of the potential parameters governing the mechanism of the transport process and whether the superexchange and incoherent hopping transport mechanisms coexist or exclude each other.

One way to experimentally determine the transfer mechanism is to measure the charge accumulation in the bridge state. In the case that the charge accumulation is detected in the bridge redox state, the incoherent hopping mechanism is clearly confirmed. On the contrary, without a noticeable amount of charge accumulated in the bridge state, the transport mechanism remains inconclusive. Even if an electron is in fact transported through incoherent hopping pathways, it may be difficult to detect the electronic population in a bridge state if the lifetime of the electronic reduction of the bridge state is much shorter than the characteristic time of the transport process. The dynamics occur especially when the coupling between the bridge and acceptor states is very strong such that an electron hops to an acceptor state as soon as the electronic accumulation occurs on the bridge. Furthermore, it is obvious that the superexchange transport does not allow charge accumulation in a bridge state. Therefore, bridges with no charge accumulation can support either superexchange or incoherent hopping mechanism. The situation is similar with theoretical studies. To resolve this issue, one should be able to separate one mechanism from the other and to isolate the contribution of an individual pathway to the electronic transport.

In this letter, we present the Feynman and Vernon's path integral scheme[7] that provides a valuable tool for decomposing the reduced density matrix of the system into partial density matrices that correspond to different transport mechanisms. The letter is organized as follows: In section 2, we discuss the path integral formalism in which pathways are classified into different transport mechanisms and the contribution of each pathway is analyzed. In section 3, the method is applied to simple ET systems, followed by concluding remarks in section 4.

2. Methodology

For ET systems and devices, a straightforward way to keep track of the dynamics of electrons traveling from donor to acceptor is to calculate the time evolution of the diagonal elements of the density matrix of the system that is expressed in the local state representation. Feynman's path integral formalism on a system coupled to baths is advantageous for this purpose because the reduced density matrix only depends on the system coordinates including baths inherently after Gaussian integration of bath degrees of freedom. In particular, selecting a local state representation which physically describes the electronic sites involved in electronic transport allows direct comparison between the simulated density matrix and experimental measurements of electronic accumulation. For the problem of ET, optimal local states correspond to the reduced electronic states of donors, bridges, and acceptors. Following Feynman and Vernon,[7] the discretized path integral expression of the reduced density matrix takes the form of the system propagator (**S**) multiplied by the influence functional (**I**) such that

$$\tilde{\rho}(t) = \sum_i \mathbf{S}(\Gamma_i^{(N)}; t)\, \mathbf{I}(\Gamma_i^{(N)}; t) \qquad (1)$$

where the summation runs for all possible pathways connecting

* Corresponding author. E-mail: esim@yonsei.ac.kr. Fax: +82-2-364-7050.

10.1021/jp045641l CCC: $27.50
Published on Web 11/19/2004

the donor and acceptor local states and $\Gamma_i^{(N)}$ represents the path segment from time 0 to $N\Delta t = t$ that belongs to the ith pathway. As is well-known, the system propagator includes the initial system density matrix and the low-dimensional forward and backward bare system short-time propagators, while the influence functional arises from the coupling to the environment. The closed form of the influence functional integral exists only for the very special case of harmonic baths with linear coupling. For nonlinear coupling, on the other hand, the influence functional cannot be computed analytically even with a harmonic bath. However, if the coupling is weak and the anharmonicity is insignificant, the influence functional can be calculated perturbatively.[8]

Recently, an extremely efficient way of propagating the quantum mechanical reduced density matrix for systems embedded in condensed media has been developed.[9] The details of the methodology can be found in ref 9. The influence functional in eq 1 includes the interactions that are nonlocal in time. Owing to the bath memory terms, the system propagator and the influence functional are rewritten such that the reduced density matrix is expressed as a product of *history* and *memory* terms.

$$\tilde{\rho}(t) = \sum_i \mathbf{T}(\Gamma_i^{(N-1)})\, \mathbf{P}^e(\Gamma_i^{(N)}) \tag{2}$$

Notice that the history term only depends on the past time points from 0 to $t - \Delta t$; in contrast, the memory term includes the interactions between the present time point and the past time points. By identifying the history and the memory terms, a substantial amount of redundant evaluations of interactions between history points can be omitted. Furthermore, the strength of nonlocal interactions due to the dissipative environments drops off rapidly, implying that only a finite memory length needs to be included. Furthermore, due to the artificial memory cutoff, some of the paths are in fact identical, which allows the history weights of such indistinguishable segments to be combined as one effective pathway. Nevertheless, up to the bath memory time, the number of configurations to be integrated increases exponentially. To alleviate the computational difficulty, the filtering of the propagator functional is applied. As a result, on-the-fly filtering substantially reduces the number of paths to be integrated.

The summation of all the paths in eq 1 is equivalent to multidimensional integration of the discretized time points. Regardless of the number of bridges that exist between donor and acceptor, electrons hop from one site to its nearest neighbors by taking sequential pathways, while electrons take a direct route from donor to acceptor in superexchange pathways. To elucidate the transport mechanism, we classify paths into incoherent hopping, coherent superexchange, static, and mixed pathways. Therefore, the reduced density matrix of the system is decomposed to contributions of the pathways

$$\tilde{\rho}(t) = \tilde{\rho}^{\mathrm{i}}(t) + \tilde{\rho}^{\mathrm{c}}(t) + \tilde{\rho}^{\mathrm{s}}(t) + \tilde{\rho}^{\mathrm{m}}(t) \tag{3}$$

where the superscripts i, c, s, and m stand for incoherent hopping, coherent superexchange, static, and mixed pathways, respectively. A static pathway refers to the path that does not move from its initial state, while the mixed pathways include paths that make incoherent and coherent jumps between states. Through the classification of pathways, one can see that each pathway contributes to the full density matrix elements and is uncorrelated with other pathways, allowing independent computation of the path integration of each mechanism. The summation over contributions of all four pathways may be performed to ensure the validity of the calculation.

TABLE 1: Energies of the Bridge and Acceptor States of Electron Transfer Systems and the Electronic Coupling Constants between Donor and Bridge (V_{12}) and Bridge and Acceptor (V_{23})[a]

configuration	E_2 (cm^{-1})	E_3 (cm^{-1})	V_{12} (cm^{-1})	V_{23} (cm^{-1})
C1[b]	−400	−630	22	22
C2	40000	−630	270	600
C3[c]	500	−400	22	135

[a] The energy of the donor state is set as a reference, and the electronic coupling between donor and acceptor is chosen to be zero. [b] This parameter was adapted from ref 11 to represent the mutant with modified acceptor pigments of ref 12. [c] This parameter was adapted from ref 11 to represent the double mutant with modified bridge and acceptor pigments of ref 13.

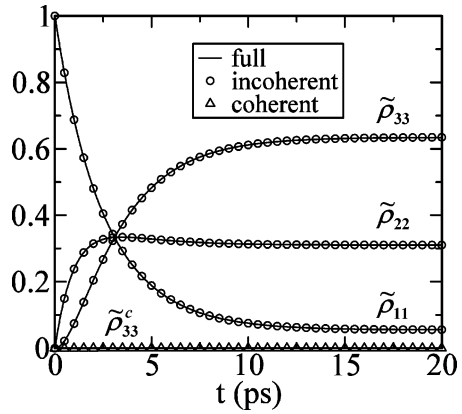

Figure 1. Three diagonal elements of the reduced density matrix ($\tilde{\rho}_{11}$ for the donor, $\tilde{\rho}_{22}$ for the bridge, and $\tilde{\rho}_{33}$ for the acceptor) of C1 configuration in Table 1 obtained by including all pathways ($\tilde{\boldsymbol{\rho}}(t)$, solid lines) and by only including incoherent hopping pathways ($\tilde{\boldsymbol{\rho}}^{\mathrm{i}}(t)$, circles). The acceptor state population transferred by coherent superexchange pathways ($\tilde{\rho}_{33}{}^{\mathrm{c}}(t)$, triangles) is also shown but negligible. $\tilde{\boldsymbol{\rho}}(t)$ and $\tilde{\boldsymbol{\rho}}^{\mathrm{i}}(t)$ are indistinguishable. This verifies that the transport process with C1 configuration is dominated by the incoherent hopping mechanism and that the superexchange mechanism is excluded.

3. Discussion

In this section, we present numerical results of simple ET systems. The charge transfer process in the well-known photosynthetic purple bacterial reaction center was taken for the purpose of benchmarking.[10,11] The system consists of three redox states, donor, bridge, and acceptor, that are embedded in baths. For this particular biological system, electronic coupling constants between redox states and their energies have been intensively investigated in many studies. The parameters including the Ohmic spectral density of the bath were adapted from ref 11. The tight-binding parameters are summarized in Table 1. The C1 configuration corresponds to the single mutant with modified acceptor pigments,[12] which has a low-lying bridge state. It can be easily predicted that the ET within such a configuration is dominated by the incoherent hopping mechanism and that the calculated full reduced density matrix ($\tilde{\boldsymbol{\rho}}(t)$) and the contribution of incoherent pathways ($\tilde{\boldsymbol{\rho}}^{\mathrm{i}}(t)$) should essentially be identical. This is clearly indicated from our results in Figure 1 where the three diagonal elements of the propagated reduced density matrix ($\tilde{\rho}_{11}$ for the donor, $\tilde{\rho}_{22}$ for the bridge, and $\tilde{\rho}_{33}$ for the acceptor), that represent the time evolution of the electronic occupation of states, coincide with those of the incoherent contribution indistinguishably. The acceptor popula-

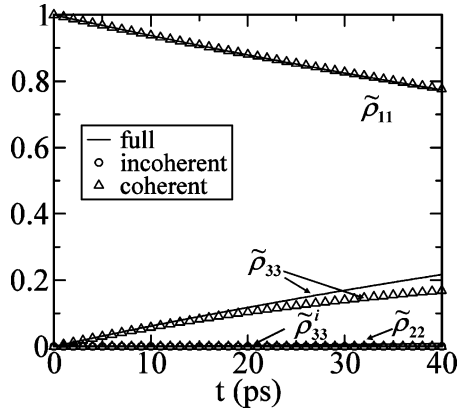

Figure 2. Three diagonal elements of the reduced density matrix ($\tilde{\rho}_{11}$ for the donor, $\tilde{\rho}_{22}$ for the bridge, and $\tilde{\rho}_{33}$ for the acceptor) of C2 configuration in Table 1 obtained by including all pathways ($\tilde{\boldsymbol{\rho}}(t)$, solid lines) and by only including coherent superexchange pathways ($\tilde{\boldsymbol{\rho}}^{c}(t)$, triangles). The acceptor state population transferred by incoherent hopping pathways ($\tilde{\rho}_{33}^{i}(t)$, circles) is also shown but negligible. $\tilde{\boldsymbol{\rho}}(t)$ and $\tilde{\boldsymbol{\rho}}^{c}(t)$ agree very well. This verifies that the transport process with C2 configuration is dominated by the coherent superexchange mechanism.

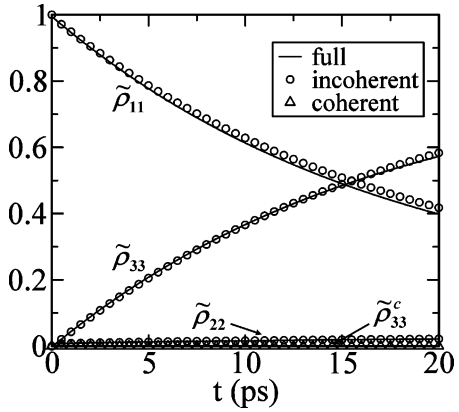

Figure 3. Same as Figure 1 with C3 configuration in Table 1.

tion due to coherent superexchange transport ($\tilde{\rho}_{33}^{c}(t)$) has also been plotted, which is negligible for the duration of simulation time.

To verify that the method is equally valid for a superexchange case, we configured C2 such that electrons take a direct route to an acceptor state. In addition, to make sure that the transport occurs via superexchange pathways, we set direct electronic coupling constants between donor and acceptor to be equal to zero. Therefore, the effective coupling between donor and acceptor is only provided through a virtual bridge. Figure 2 shows the propagated electronic population of three redox states in the C2 system. To induce substantial population transfer to the acceptor state within the simulation time, 40 ps, large values were selected for the electronic coupling constants. It should be noted that the three diagonal elements of the full reduced density matrix and corresponding matrix elements of the coherent pathway contribution are in excellent agreement. Small discrepancy between $\tilde{\rho}_{33}(t)$ and $\tilde{\rho}_{33}^{c}(t)$ is due to the ignored mixed pathway contribution. The cases shown in Figures 1 and 2 corroborate that the method introduced in this letter is valid for separating the incoherent hopping and coherent superexchange pathways.

For C2, it is straightforward to predict that the superexchange pathway dominates, owing to the extremely high bridge-state energy. For most ET systems with intermediate high-energy bridges, however, it is always confusing to determine the type of transfer, since the superexchange and incoherent hopping mechanisms are equally likely. The double mutant of Heller et al.[13] has a high-energy bridge state at 500 cm^{-1}, and experimentally, no measurable electronic population on the bridge was observed. While accurate determination of the mechanism at work was impossible given the insufficient information available, we applied the new scheme to the C3 configuration to represent Heller *et al.'s* double mutant as in ref 11. Simulations revealed that it was in fact incoherent hopping dominated transport, as shown in Figure 3.

4. Concluding Remarks

The main focus of this letter was to devise a theoretical tool that unravels whether a particular ET reaction occurs via the incoherent hopping or coherent superexchange mechanism. By classifying the paths summed in Feynman's path integral formulation and by independently integrating each of the paths, it was possible to separate partial contributions of different mechanisms to ET. Two ET systems dominated by the superexchange and incoherent hopping mechanisms, respectively, were presented to verify the validity of the method along with an ET system governed by the incoherent hopping mechanism despite the high-energy bridge state. This scheme is highly useful for studying quantum mechanical transport processes and is expected to contribute significantly to the design and development of nanoelectronic devices.

Acknowledgment. This work was partly supported by the young faculty fellowship of Yonsei University. We acknowledge the support from KISTI (Korea Institute of Science and Technology Information) under "The Sixth Strategic Supercomputing Support Program". The use of the computing system of the Supercomputing Center is also greatly appreciated.

References and Notes

(1) Lambert, C.; Nöll, G.; Schelter, J. *Nat. Mater.* **2002**, *1*, 69.
(2) Imahori, H.; Yamada, H.; Nishimura, Y.; Yamazaki, I.; Sakata, Y. *J. Phys. Chem. B* **2000**, *104*, 2099.
(3) Davis, W. B.; Svec, W. A.; Ratner, M. A.; Wasielewski, M. R. *Nature* **1998**, *396*, 60.
(4) Herz, T.; Gedeck, P.; Clark, T. *J. Am. Chem. Soc.* **1999**, *121*, 1379.
(5) Giese, B. *Acc. Chem. Res.* **2000**, *33*, 631.
(6) Segal, D.; Nitzan, A.; Davis, W. B.; Wasielewski, M. R.; Ratner, M. A. *J. Phys. Chem. B* **2000**, *104*, 3817.
(7) Feynman, R. P.; Vernon, F. L., Jr. *Ann. Phys.* **1963**, *24*, 118.
(8) Makri, N. *J. Phys. Chem. B* **1999**, *103*, 2823.
(9) Sim, E. *J. Chem. Phys.* **2001**, *115*, 4450.
(10) Makri, N.; Sim, E.; Makarov, D. E.; Topaler, M. *Proc. Natl. Acad. Sci. U.S.A.* **1996**, *93*, 3926.
(11) Sim, E.; Makri, N. *J. Phys. Chem. B* **1997**, *101*, 5446.
(12) Huber, H.; Meyer, M.; Nagele, T.; Hartl, I.; Scheer, H.; Zinth, W. *J. Chem. Phys.* **1995**, *197*, 297.
(13) Heller, B. A.; Holten, D.; Kirmaier, C. *Science* **1995**, *269*, 940.